

An analysis and experimental validation of natural frequencies of elastic ellipsoids with the Rayleigh–Ritz method

Original

An analysis and experimental validation of natural frequencies of elastic ellipsoids with the Rayleigh–Ritz method / Wu, Jinghui; Wang, Ji; Xie, Longtao; Zhgoon, Sergei; Wu, Rongxing; Zhang, Aibing; Ma, Tingfeng; Du, Jianke. - In: MECHANICS OF ADVANCED MATERIALS AND STRUCTURES. - ISSN 1537-6532. - (2022).
[10.1080/15376494.2022.2077486]

Availability:

This version is available at: 11583/2978272 since: 2023-05-02T11:31:13Z

Publisher:

Taylor & Francis

Published

DOI:10.1080/15376494.2022.2077486

Terms of use:

This article is made available under terms and conditions as specified in the corresponding bibliographic description in the repository

Publisher copyright

(Article begins on next page)



An analysis and experimental validation of natural frequencies of elastic ellipsoids with the Rayleigh–Ritz method

Jinghui Wu, Ji Wang, Longtao Xie, Sergei Zhgoon, Rongxing Wu, Aibing Zhang, Tingfeng Ma & Jianke Du

To cite this article: Jinghui Wu, Ji Wang, Longtao Xie, Sergei Zhgoon, Rongxing Wu, Aibing Zhang, Tingfeng Ma & Jianke Du (2022): An analysis and experimental validation of natural frequencies of elastic ellipsoids with the Rayleigh–Ritz method, *Mechanics of Advanced Materials and Structures*, DOI: [10.1080/15376494.2022.2077486](https://doi.org/10.1080/15376494.2022.2077486)

To link to this article: <https://doi.org/10.1080/15376494.2022.2077486>



Published online: 25 May 2022.



Submit your article to this journal [↗](#)



Article views: 83





View related articles [↗](#)



View Crossmark data [↗](#)

An analysis and experimental validation of natural frequencies of elastic ellipsoids with the Rayleigh–Ritz method

Jinghui Wu^a , Ji Wang^{a,b} , Longtao Xie^{a,b}, Sergei Zhgoon^c, Rongxing Wu^{a,b}, Aibing Zhang^{a,b}, Tingfeng Ma^{a,b}, and Jianke Du^a

^aPiezoelectric Device Laboratory, School of Mechanical Engineering & Mechanics, Ningbo University, Ningbo, Zhejiang, China; ^bTXC-NBU Joint Center of Research, School of Mechanical Engineering & Mechanics, Ningbo University, Ningbo, Zhejiang, China; ^cMoscow Power Engineering Institute, Moscow, Russia

ABSTRACT

The Rayleigh–Ritz method is widely employed to analyze free vibrations of elastic solids and structures. For a simple formulation and efficient evaluation of vibrations of elastic ellipsoids, which also include spheres, the Cartesian coordinate system is utilized. It is hoped that the formulation with lengthy expressions can be solved with fewer terms of displacement functions in Chebyshev polynomials for simple evaluations of stiffness and mass matrices of the elastic ellipsoids with the procedure. The vibrations of elastic ellipsoids are calculated with geometric parameters for the validation of the procedure and formulation with known results and the analysis from this study.

ARTICLE HISTORY

Received 10 May 2022
Accepted 10 May 2022

KEYWORDS

Rayleigh–Ritz method; vibration; ellipsoid; frequency; Chebyshev; polynomials; mode

1. Introduction

There are many natural and artificial solids with perfect geometric configurations such as ellipsoids as objects we have to deal with in our lives daily [1, 2]. There have been many numerical approaches, such as Godunov's discrete-orthogonalization method [3], the finite element method [4, 5], the Rayleigh–Ritz method [6], among others, applied to the vibration analysis to determine the natural frequencies and vibration modes of the isotropic elastic spheres. In general, such analytical methods are widely used for the analysis of vibrations of the isotropic elastic spheres [7–9] while an exact solution to the free vibrations of elastic ellipsoids, which can also cover the usual spheres, is not available. With the existing approaches, the Rayleigh–Ritz method has been widely utilized to construct the equation of characteristic frequency of the structure with a better approximation [10–14]. The admissible functions of the displacements directly related to the convergence and the precision of the results, such as the ordinary or orthogonal polynomials, trigonometric functions [15], and so on are specifically chosen to represent the deformation with accuracy. With the minimization of the total energy functional, which involves the potential and kinetic energies of the system, the natural frequencies and mode shapes of the structure can then be obtained numerically [3].

Clearly, a sphere as a special ellipsoid has been calculated by analytical methods and measured from various experiments such as the resonant spherical technique [4, 16]. In such analyses, Hashemi and Anderson [15] adopted the spherical coordinates to study the torsional vibrations of the isotropic elastic sphere, and Deneville et al. [16]

investigated spheroidal modes of the isotropic sphere with resonant ultrasound spectroscopy (RUSpec), which is a useful measurement technique for obtaining the full range of the material properties of elastic solids with different geometries. Buchanan and Ramirez [4] worked on the vibrations of transversely isotropic solid spheres. Wang and Ding [6] studied the radial vibration of a multilayered piezoelectric/magnetostrictive composite hollow sphere.

If the structural geometry is complicated, such as an ellipsoid, it is hard to access the solution by the analytical method [3], then an approximate method such as the Rayleigh–Ritz method is a good tool that can be used to calculate the vibration properties of such an elastic structure [10, 17–23]. As it is widely known, the basis function of the Rayleigh–Ritz method has wide options, like the orthogonal polynomials [24], trigonometric functions [17], and other similar functions.

For an isotropic sphere, there are extensive research on the analysis [5, 7, 16, 25, 26], but the research on elastic ellipsoids, which are more versatile as spheric samples, is limited. In this article, the Rayleigh–Ritz method is used to calculate the natural frequencies of free vibrations of elastic ellipsoids with the Chebyshev polynomials as the basis functions. With the solution process, several examples of spheres are chosen to make comparisons using the analytical results and measurements obtained by the RUSpec technique and those obtained by the calculations of FEM. The Rayleigh–Ritz method is used to improve the accuracy of the calculations by increasing the number of terms of displacement functions. As it is found from calculations of

Table 1. The relationship between the tensor subscripts of elastic constants.

$ij(kl)$	11	22	33	23	13	12
$m(n)$	1	2	3	4	5	6

FEM, the Rayleigh–Ritz method can be used to obtain the results with same accuracy at a smaller computational cost. Then the calculated results of free vibrations of the elastic sphere are compared with the results from Oda [27] to ensure the accuracy of the method. It has been shown that the Rayleigh–Ritz technique can be used to predict vibration modes of an ellipsoid accurately. For the analysis of such a three-dimensional solid, it has a greater advantage in terms of computational time.

In summary, after reviewing methods and techniques for the analysis of natural frequencies of elastic ellipsoids, the Rayleigh–Ritz method is chosen with the basis functions in Chebyshev polynomials [13, 28]. As a cautious procedure, the analyses are done in combinations of isotropic, anisotropic, spheres, and ellipsoids respectively with rigorous validations through known results and measurements as a rare example of completeness. Eventually, it is concluded that the Rayleigh–Ritz method with Chebyshev polynomials as basis functions can analyze the free vibrations of elastic ellipsoids with a simple procedure for accurate frequency and mode shape solutions. Of course, as intended, the approximate results have been validated with RUSpec measurements satisfactorily [29–32]. The motivation of this study is to provide an approximate technique for the accurate and efficient analysis of natural frequencies of ellipsoids in conjunction with the applications of RUSpec measurements for material properties, because the evaluation libraries are better to cover all possible configurations of material samples as part of the test procedure. In addition to usual samples like cuboids, cylinders, and spheres [33, 34], this research is planned to include more adaptable configurations such as ellipsoids, cones, pyramids, prisms, polyhedrons, among others, with possible truncations so most samples can be prepared from originals with minimal cost and impact due to processing. This, of course, is consistent with the general principle of the RUSpec testing, and it is more desirable to have an ellipsoid first because it can cover many variations of spheric samples with further considerations of possible truncations and alternations. Clearly, the analysis of ellipsoidal objects is an important part of the improvement and enhancement of RUSpec sample library with more analytical data for comparison and iteration. The application of the Rayleigh–Ritz method has been refined with the validated basis functions and experimental verification through actual measurements of ellipsoidal samples. The work presented in this article will certainly provide further guidance and encouragements for the development of RUSpec with suitable tools and clear path for broader and easy applications.

2. The Rayleigh–Ritz method formulation

2.1. The analysis of an elastic ellipsoid

Assuming that a homogeneous elastic ellipsoid is shown in Figure 1 with a Cartesian coordinate system and its center is

at the origin. Let a , b and c are the principal semiaxes, implying the equation of such an ellipsoid is

$$\frac{x^2}{a^2} + \frac{y^2}{b^2} + \frac{z^2}{c^2} = 1. \quad (1)$$

If $a = b = c$, it becomes a sphere.

For the vibration analysis of the ellipsoid by the Rayleigh–Ritz method, the required strain energy in strain tensors is

$$V = \frac{1}{2} \int_V \varepsilon_{ij} C_{ijkl} \varepsilon_{kl} dV, \quad i, j, k, l = 1, 2, 3, \quad (2)$$

where ε_{ij} and C_{ijkl} are the second-order strain tensor and the fourth-order tensor of elastic constants of the material with a volume of V , respectively. For the simplification of the calculation, the contracted notations of the second-order tensor are used for the elastic constants, which have the correspondence between the fourth-order tensor with the relationship shown in Table 1 [34].

If the material is isotropic, $C_{11} = C_{22} = C_{33} = \lambda + 2\mu$, $C_{12} = C_{13} = \lambda$, $C_{44} = C_{55} = C_{66} = \mu$ with $\lambda = E\nu/(1 + \nu)(1 - 2\nu)$ and $\mu = E/2(1 + \nu)$, and E represents the Young's model and ν is the Poisson's ratio of material. For the linear deformation of vibrations, with displacements u_i ($i = 1, 2, 3$), the strain tensors are

$$\begin{aligned} \varepsilon_{11} &= \frac{\partial u_1}{\partial x_1} = u_{1,1}, \quad \varepsilon_{22} = \frac{\partial u_2}{\partial x_2} = u_{2,2}, \quad \varepsilon_{33} = \frac{\partial u_3}{\partial x_3} = u_{3,3}, \\ \varepsilon_{12} &= \varepsilon_{21} = \frac{\partial u_1}{\partial x_2} + \frac{\partial u_2}{\partial x_1} = u_{1,2} + u_{2,1}, \\ \varepsilon_{13} &= \varepsilon_{31} = \frac{\partial u_1}{\partial x_3} + \frac{\partial u_3}{\partial x_1} = u_{1,3} + u_{3,1}, \\ \varepsilon_{23} &= \varepsilon_{32} = \frac{\partial u_2}{\partial x_3} + \frac{\partial u_3}{\partial x_2} = u_{2,3} + u_{3,2}. \end{aligned} \quad (3)$$

Similarly, the kinetic energy is

$$T = \frac{1}{2} \int_V \rho \dot{u}_i \dot{u}_i dV, \quad l = 1, 2, 3, \quad (4)$$

where ρ is density of material.

As it has been stated before, the critical factor of the accuracy of the Rayleigh–Ritz method is relying on the choice of displacement functions. Generally speaking, if the chosen displacements satisfy the boundary conditions of the physical problem, the vibration solutions will converge fast and achieve better accuracy. With earlier studies on the general implementation of the Rayleigh–Ritz method, we follow the recommendations based on earlier studies with good results by expanding displacement functions with Chebyshev polynomials as

$$\begin{aligned} u_1 &= U_1 e^{i\omega t} = \sum_{l=1}^L \sum_{m=1}^M \sum_{n=1}^N A_{lmn} P_l(x) P_m(y) P_n(z) e^{i\omega t} \\ u_2 &= U_2 e^{i\omega t} = \sum_{o=1}^O \sum_{p=1}^P \sum_{q=1}^Q B_{eos} P_e(x) P_o(y) P_s(z) e^{i\omega t} \\ u_3 &= U_3 e^{i\omega t} = \sum_{r=1}^R \sum_{s=1}^S \sum_{t=1}^T C_{fgh} P_f(x) P_g(y) P_h(z) e^{i\omega t} \end{aligned} \quad (5)$$

where ω is the angular frequency, A_{lmn} , B_{eos} , C_{fgh} are displacement amplitudes, $P_l(x)$ ($P_e(x)$, $P_f(x)$), $P_m(y)$ ($P_o(y)$, $P_g(y)$), and $P_n(z)$ ($P_s(z)$, $P_h(z)$) denote the assumed admissible functions in the x -, y -, and z - directions, respectively. The boundary range $x = \pm a$, $y = \pm b$, $z = \pm c$ are the intercepts of the ellipsoid in the x -, y - and z - directions, ω is the angular frequency of the vibrations, and t is time, respectively. The basis functions here are the Chebyshev polynomials [34]

$$\begin{aligned} P_0(x) &= 1, \\ P_1(x) &= x, \\ &\dots \\ P_n(x) &= 2xP_{n-1}(x) - P_{n-2}(x), \quad n \geq 2, \end{aligned} \quad (6)$$

where n is the order of the polynomial.

2.2. Modal characteristics by the Rayleigh–Ritz method

The energy expressions will give the Lagrangian of the vibrating ellipsoid as

$$\Lambda = T_{\max} - V_{\max}. \quad (7)$$

According to the principle of conservation of energy, $T_{\max} = V_{\max}$, and the known displacements, the maximum energies from Eqs. (2) and (4) are

$$V_{\max} = \frac{1}{2} \int_V U_{i,j} C_{ijkl} U_{k,l} dV, \quad i, j, k, l = 1, 2, 3, \quad (8)$$

$$T_{\max} = \frac{\rho\omega^2}{2} \int_V U_i^2 dV, \quad i = 1, 2, 3. \quad (9)$$

To make the expression simpler, all the following representations in this section are with the consideration of the symmetric modes only. Applying the variational principle, the following equations can be obtained from Eq. (7)

$$\frac{\partial \Lambda}{\partial A_{lmn}} = 0, \quad \frac{\partial \Lambda}{\partial B_{eos}} = 0, \quad \frac{\partial \Lambda}{\partial C_{fgh}} = 0, \quad (10)$$

which result in a typical eigenvalue problem

$$\mathbf{KA} - \omega^2 \mathbf{MA} = 0. \quad (11)$$

The matrices \mathbf{K} and \mathbf{M} are assembled as the stiffness and mass matrices, respectively, and \mathbf{A} is the column vector of the unknown amplitude coefficients (A_{lmn} , B_{eos} , C_{fgh}) of deformation.

The eigenvalue problem of Eq. (11) can be written as

$$\left(\begin{bmatrix} \mathbf{K}_{U_1 U_1} & \mathbf{K}_{U_1 U_2} & \mathbf{K}_{U_1 U_3} \\ \mathbf{K}_{U_1 U_2}^T & \mathbf{K}_{U_2 U_2} & \mathbf{K}_{U_2 U_3} \\ \mathbf{K}_{U_1 U_3}^T & \mathbf{K}_{U_2 U_3}^T & \mathbf{K}_{U_3 U_3} \end{bmatrix} - \omega^2 \begin{bmatrix} \mathbf{M}_{U_1 U_1} & 0 & 0 \\ 0 & \mathbf{M}_{U_2 U_2} & 0 \\ 0 & 0 & \mathbf{M}_{U_3 U_3} \end{bmatrix} \right) \times \begin{Bmatrix} \{\mathbf{A}\} \\ \{\mathbf{B}\} \\ \{\mathbf{C}\} \end{Bmatrix} = \begin{Bmatrix} 0 \\ 0 \\ 0 \end{Bmatrix}. \quad (12)$$

The stiffness and mass matrices \mathbf{K} and \mathbf{M} are obtained by substituting U_i into Eq. (12) for elements

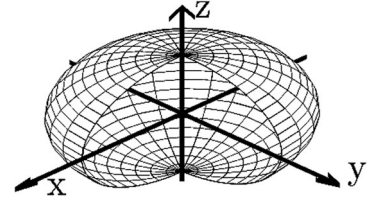


Figure 1. A homogeneous elastic ellipsoid.

$$\begin{aligned} \mathbf{K}_{U_i U_k} &= c_{i1k1} E_{U_i p U_k \bar{p}}^{1,1} F_{U_i q U_k \bar{q}}^{0,0} G_{U_i r U_k \bar{r}}^{0,0} + c_{i1k2} E_{U_i p U_k \bar{p}}^{1,0} F_{U_i q U_k \bar{q}}^{0,1} G_{U_i r U_k \bar{r}}^{0,0} \\ &+ c_{i1k3} E_{U_i p U_k \bar{p}}^{1,0} F_{U_i q U_k \bar{q}}^{0,0} G_{U_i r U_k \bar{r}}^{0,1} + c_{i2k1} E_{U_i p U_k \bar{p}}^{0,1} F_{U_i q U_k \bar{q}}^{1,0} G_{U_i r U_k \bar{r}}^{0,0} \\ &+ c_{i2k2} E_{U_i p U_k \bar{p}}^{0,0} F_{U_i q U_k \bar{q}}^{1,1} G_{U_i r U_k \bar{r}}^{0,0} + c_{i2k3} E_{U_i p U_k \bar{p}}^{0,0} F_{U_i q U_k \bar{q}}^{1,0} G_{U_i r U_k \bar{r}}^{0,1} \\ &+ c_{i3k1} E_{U_i p U_k \bar{p}}^{0,1} F_{U_i q U_k \bar{q}}^{0,0} G_{U_i r U_k \bar{r}}^{1,0} + c_{i3k2} E_{U_i p U_k \bar{p}}^{0,0} F_{U_i q U_k \bar{q}}^{0,1} G_{U_i r U_k \bar{r}}^{1,0} \\ &+ c_{i3k3} E_{U_i p U_k \bar{p}}^{0,0} F_{U_i q U_k \bar{q}}^{0,0} G_{U_i r U_k \bar{r}}^{1,1}, \end{aligned} \quad (13)$$

$$\mathbf{M}_{U_i U_k} = \rho E_{U_i p U_k \bar{p}}^{0,0} F_{U_i q U_k \bar{q}}^{0,0} G_{U_i r U_k \bar{r}}^{0,0}, \quad (14)$$

where

$$\begin{aligned} E_{U_i p U_k \bar{p}}^{\alpha, \beta} &= a \int_{-1}^1 \frac{d^\alpha P_p(X)}{dX^\alpha} \frac{d^\beta P_{\bar{p}}(X)}{dX^\beta} dX, \\ F_{U_i q U_k \bar{q}}^{\alpha, \beta} &= b \int_{-\sqrt{1-X^2}}^{\sqrt{1-X^2}} \frac{d^\alpha P_q(Y)}{dY^\alpha} \frac{d^\beta P_{\bar{q}}(Y)}{dY^\beta} dY, \\ G_{U_i r U_k \bar{r}}^{\alpha, \beta} &= c \int_{-\sqrt{1-X^2-Y^2}}^{\sqrt{1-X^2-Y^2}} \frac{d^\alpha P_r(Z)}{dZ^\alpha} \frac{d^\beta P_{\bar{r}}(Z)}{dZ^\beta} dZ. \end{aligned} \quad (15)$$

In the above equations, α and β are the order of the derivatives, p , q , r , \bar{p} , \bar{q} and \bar{r} are the order of the polynomials, where p , $\bar{p} = l, e, f$; $q, \bar{q} = m, o, g$; $r, \bar{r} = n, s, h$, and the normalized variables to simplify the calculations are $X = x/a$, $Y = y/b$, $Z = z/c$. The elements of \mathbf{K} and \mathbf{M} above are actually $[K_{U_i U_j}]_{mn}$ and $[M_{U_i U_j}]_{mn}$ with $m = r + (q - 1)L + (p - 1)L^2$, $n = \bar{r} + (\bar{q} - 1)L + (\bar{p} - 1)L^2$. Through the Eq. (12), the angular frequency ω and the associated eigenvector \mathbf{A} can be obtained, then the frequency of the structure can be also obtained with $f = \omega/2\pi$. In comparison to the analytical method, it is more convenient to obtain the frequencies and mode shapes of the vibration from the eigenvalue problem.

3. Numerical results

3.1. The natural frequencies of an isotropic sphere

To illustrate the capability of the presented procedure in obtaining the frequencies and mode shapes of an elastic ellipsoid, several examples of vibration analysis of isotropic spheres are compared with results from an earlier study [7]. According to the Figures 2–5, the results have basically converged at the order of polynomials is 9 for the admissible polynomials along the three axes, respectively, and 12 has been chosen as the order for the calculation at high frequencies. More terms in the deformation series could induce formidable computational problems in the solution process, as it can be imagined.

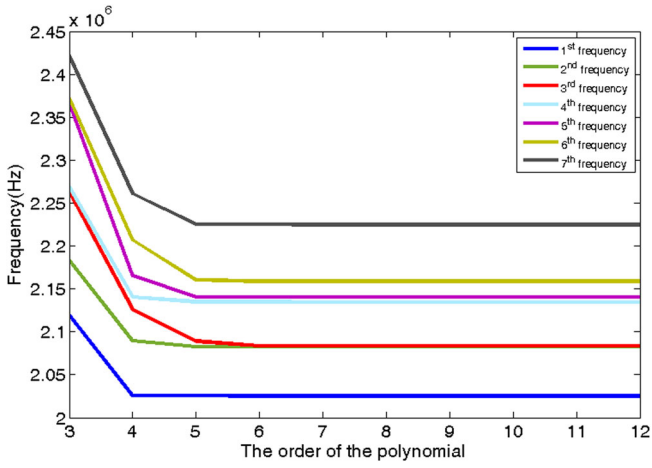


Figure 2. Convergence of an isotropic sphere with a radius of 1 mm.

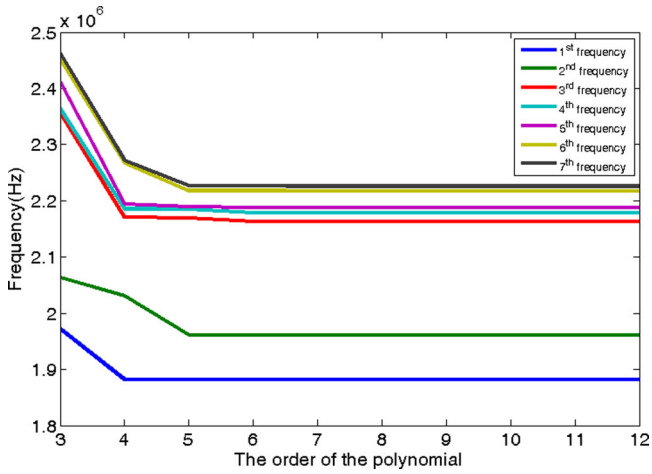
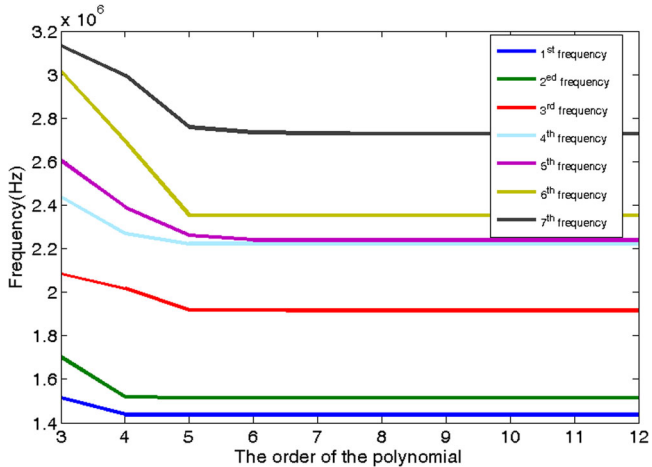
Figure 3. Convergence of an isotropic ellipsoid with $a = 1\text{ mm}$, $b = 0.9\text{ mm}$, $c = 0.8\text{ mm}$.

Figure 4. Convergence of an isotropic sphere with a radius of 1 mm.

In this study, the normalized frequency is defined as

$$C = \frac{\omega\delta}{c_T}, \quad (16)$$

where $\delta = \sqrt{abc3}$ and c_T is the transverse wave velocity of an isotropic elastic solid known as

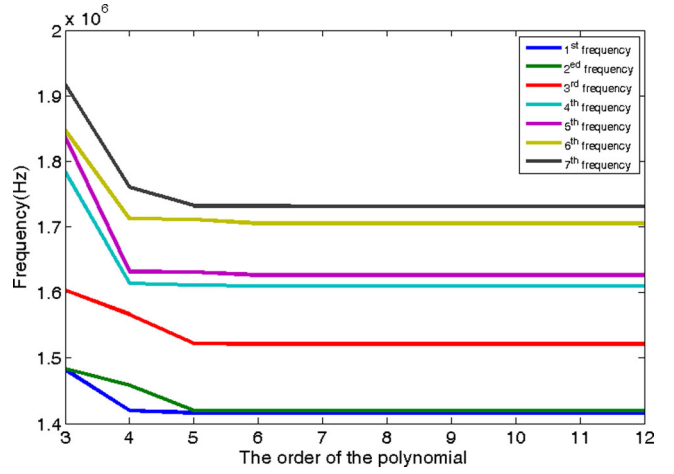
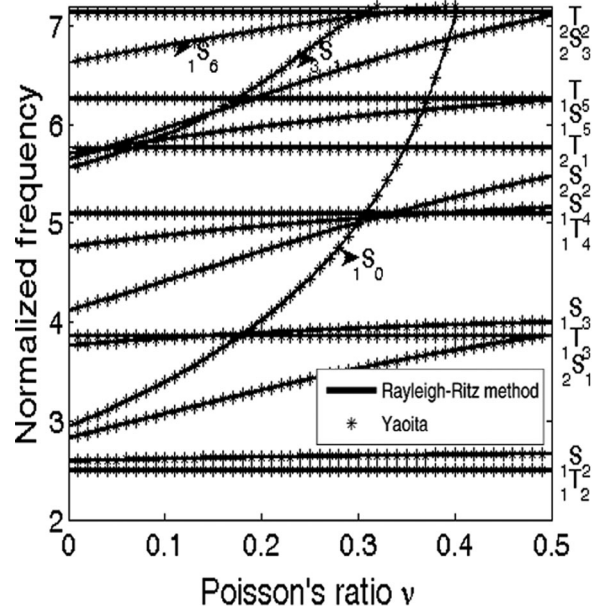
Figure 5. Convergence of an isotropic ellipsoid with $a = 1\text{ mm}$, $b = 0.9\text{ mm}$, $c = 0.8\text{ mm}$.

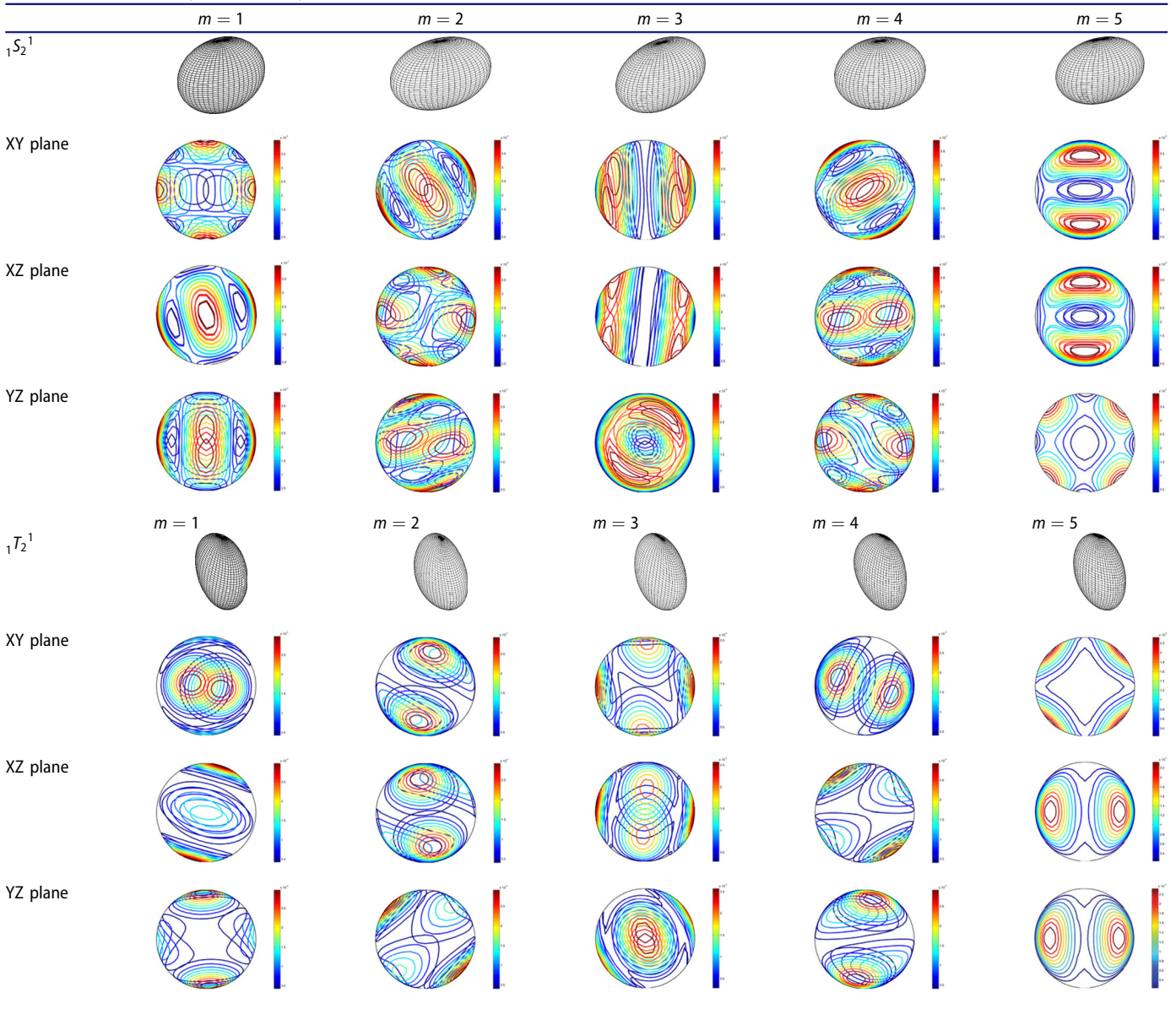
Figure 6. The relation between normalized frequencies and Poisson's ratio of an isotropic sphere.

Table 2. A comparison of frequencies from this and earlier studies.

k	Mode	This study $f(\text{MHz})$	Yaoita [7] $f(\text{MHz})$
1	$1T_2^1$	1.437	1.437
2	$1S_2^1$	1.514	1.514
3	$2S_1^2$	1.917	1.917
4	$1T_3^1$	2.221	2.221
5	$1S_3^1$	2.240	2.240
6	$1S_0^1$	2.355	2.353
7	$2S_2^2$	2.728	2.728
8	$1S_4^1$	2.860	2.860
9	$1T_4^1$	2.928	2.927
10	$2T_1^2$	3.312	3.311

$$c_T = \sqrt{\frac{\mu}{\rho}}. \quad (17)$$

If $a = b = c$, the solid is a special ellipsoid or a sphere, then the relation between normalized frequencies and Poisson's ratio of a sphere is given in Figure 6 from Eq. (12). In this figure, the spheroidal and torsional vibration modes

Table 3. Some mode shapes of a BK-7 sphere.

are denoted as ${}_iS_n$ and ${}_iT_n$ with i and n indicate the number of vibration nodes in the radial direction of the sphere and the order of spherical Bessel functions J_n , respectively [7]. Since the spherical modes are a mixture of shear and dilatational wave modes, they depend on Poisson's ratio [27]. While the torsional modes are only shear modes, they are independent of Poisson's ratio [5]. Besides, the results computed from the analytical method [7] are also shown in Figure 6, and they are in very good agreement between these two approaches can be observed.

Table 2 lists the numerical results of an elastic sphere of BK-7 glass with material and structural properties $E = 79.2\text{GPa}$, $\nu = 0.21$, $\rho = 2510\text{kg/m}^3$, $a = b = c = 1\text{mm}$ for the analyses with the Rayleigh-Ritz and other analytical methods. The largest difference among them is within 0.1%, which are much smaller than expected. The method presented in this article has some advantages like much less

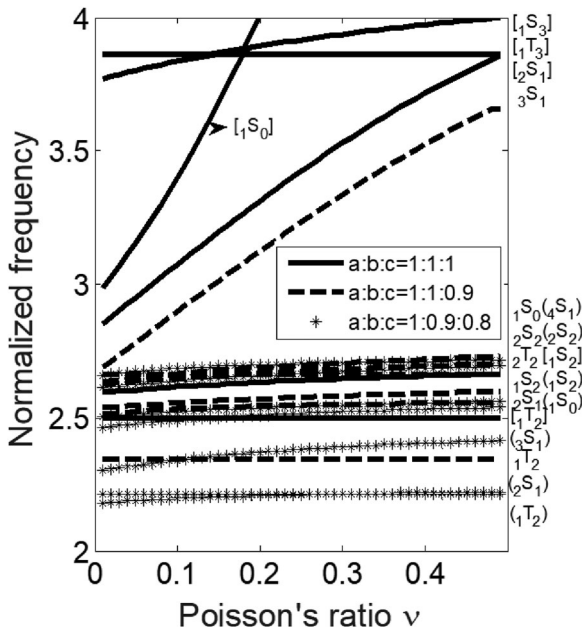
computational cost and obtaining the frequencies and mode shapes at the same time.

An ideal isotropic sphere could have different mode numbers $m(=1, 2, \dots, 2n+1)$ and the same natural frequency because of modal degeneration. There are some typical mode shapes known as ${}_1S_2$ and ${}_1T_2$ are listed in Table 3.

The measurement results also proved that the Rayleigh-Ritz method is reliable in obtaining the frequencies of the elastic solids. The five glass balls with almost same composition ingredients ($\text{SiO}_2 > 65\%$, $\text{Na}_2\text{O} > 14\%$, $\text{CaO} > 8\%$, $\text{MgO} > 2.5\%$, $\text{Al}_2\text{O}_3 > 0.5\%$, $\text{Fe}_2\text{O}_3 > 0.1\%$) and same size with $r = 5\text{mm}$ have been measured by the resonant ultrasound spectroscopy (RUSpec), which simulates the free boundary conditions by means of a resilient holding device of specimen, using an emitter to excite ultrasonic waves with gradually increasing frequency in a certain range. If the frequency of excitation coincides with the intrinsic frequency of

Table 4. A comparison of frequencies from calculation and measurement.

Properties of the ball	Frequency	RUSpec (kHz)	This study(kHz)	Errors
$E = 73.128\text{GPa}$, $\nu = 0.217$, $\rho = 2557.1\text{kg/m}^3$	1	273.01	272.89	0.041%
	2	287.93	287.53	0.139%
	3	364.49	365.64	0.313%
	4	421.55	421.67	0.028%
$E = 72.454\text{GPa}$, $\nu = 0.225$, $\rho = 2513.9\text{kg/m}^3$	1	270.93	273.06	0.779%
	2	288.10	287.83	0.093%
	3	364.63	367.83	0.870%
	4	421.79	421.93	0.033%
$E = 73.555\text{GPa}$, $\nu = 0.215$, $\rho = 2513.9\text{kg/m}^3$	1	272.26	272.35	0.035%
	2	286.60	286.93	0.113%
	3	364.66	364.42	0.067%
	4	419.92	420.84	0.217%
$E = 73.723\text{GPa}$, $\nu = 0.221$, $\rho = 2611.2\text{kg/m}^3$	1	270.16	270.70	0.200%
	2	285.59	285.28	0.107%
	3	363.70	363.68	0.001%
	4	418.09	418.29	0.046%
$E = 73.008\text{GPa}$, $\nu = 0.221$, $\rho = 2507.3\text{kg/m}^3$	1	273.42	274.91	0.545%
	2	289.83	289.72	0.039%
	3	367.08	369.34	0.611%
	4	426.52	424.79	0.404%

**Figure 7.** The relationship between normalized frequencies and Poisson's ratios of ellipsoids with different sizes.

the specimen itself, a resonance phenomenon will occur, and the receiver detects the signal and obtains the corresponding frequency. The results are shown in the Table 4.

3.2. The natural frequencies of an isotropic ellipsoid

If the three axes of the elastic solid are unequal, it is a typical ellipsoid. There are several examples of natural frequencies of an isotropic ellipsoid with the different sizes shown in Figure 7.

In comparison with spheres, because a, b, c are not equal to each other in ellipsoids, each frequency only has one mode or two modes. This means that the vibration mode shapes of the isotropic elastic ellipsoid are much less than the sphere of the same material in the frequency range. While the data in a bracket implies the mode of the ellipsoid with $a : b : c = 1 :$

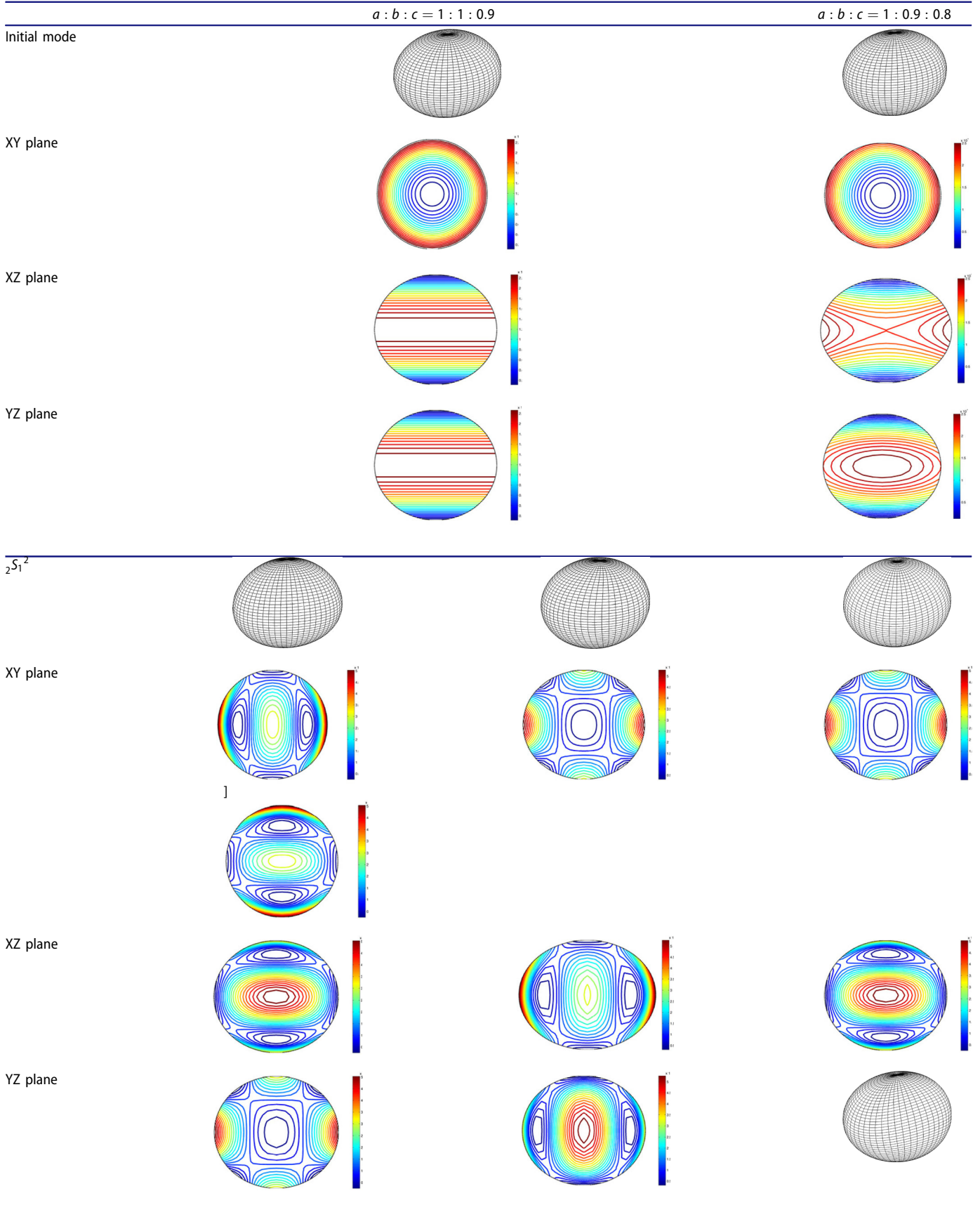
$0.9 : 0.8$, the data in square bracket represent the mode of the ellipsoid with $a : b : c = 1 : 1 : 1$, and the remaining cases meaning the mode of the ellipsoid with $a : b : c = 1 : 1 : 0.9$. Figure 7 shows that whatever the size of the ellipsoid, and the torsional modes are independent on Poisson's ratios since the torsional modes are determined by shear deformation only. Again, several modes of the ellipsoid of BK-7 glass with different sizes are shown in Table 5.

For a validation of vibration frequencies and mode shapes of ellipsoids, five ellipsoid samples were fabricated using DM12, a resin widely used in 3D printing by the SLA 3D printer (Shining3D Company, Yangzhou, Jiangsu Province, China), have been measured with the resonant ultrasound spectroscopy (RUSpec, Magnaflux Quasar Systems, Albuquerque, New Mexico, USA), and the results are shown in Table 6. It showed that calculation and measurements are close and the calculation procedure in this article can be used for material characterization with unusual and small samples, as the study is intended to.

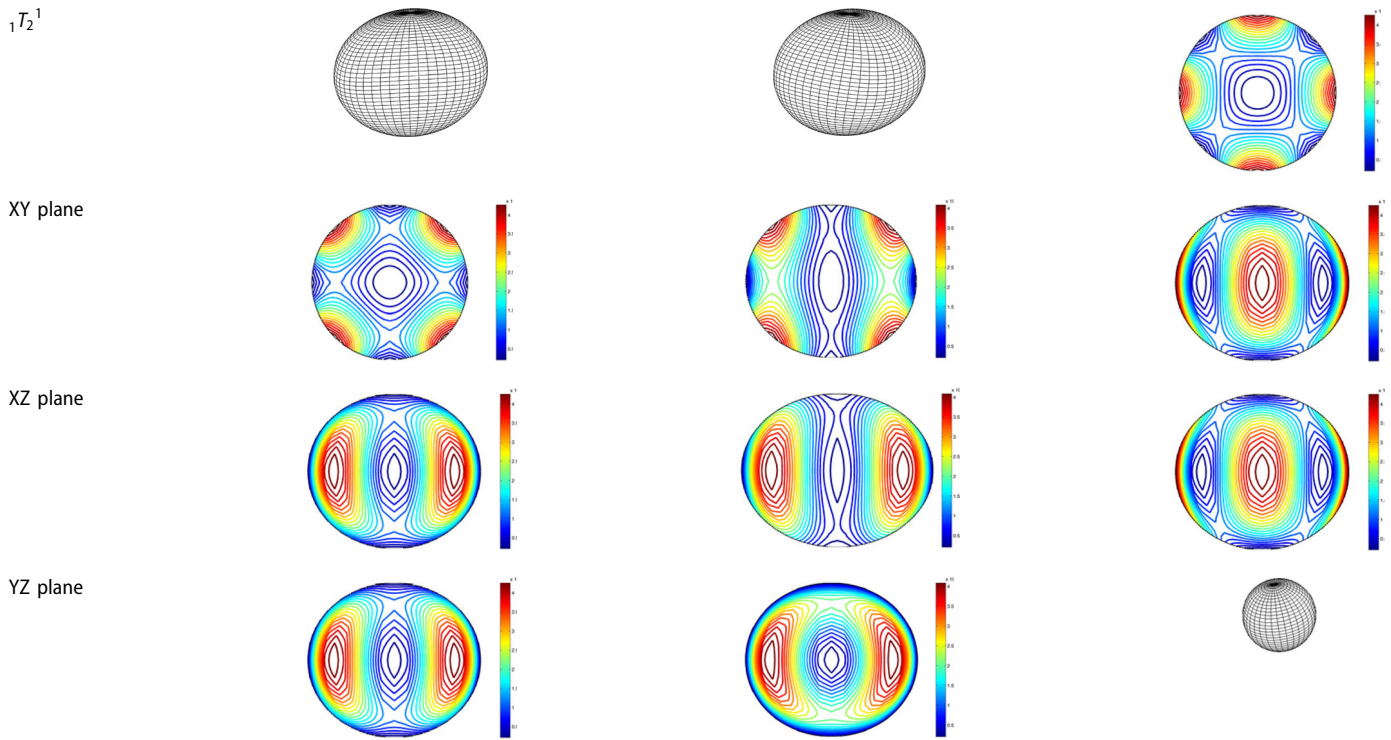
3.3. The natural frequency of an anisotropic sphere

As a further validation of the method and results, frequencies of a spherical specimen of single-crystal periclase as presented in an earlier study by Oda [33] are used for comparison in this part. In comparison to an isotropic elastic sphere, the vibration modes of anisotropic spherical with cubic crystal symmetry are much sparse. The vibration modes are divided into ten groups, such as single modes, twofold degenerate modes, and threefold degenerate modes [33]. Specifically, the mode groups are denoted as single modes (A_{1g} , A_{2g} , A_{1u} and A_{2u}), twofold degenerate modes (E_g and E_u), and threefold degenerate modes (T_{1g} , T_{2g} , T_{1u} and T_{2u}). With material properties of olivine specimen $\rho = 3.350 \times 10^3 \text{kg/m}^3$, $a = b = c = 0.893 \text{mm}$, elastic constants $C_{11} = 319.61 \text{GPa}$, $C_{12} = 69.24 \text{GPa}$, $C_{22} = 197.32 \text{GPa}$, $C_{23} = 75.67 \text{GPa}$, $C_{31} = 70.92 \text{GPa}$, $C_{33} = 236.84 \text{GPa}$, $C_{44} = 64.06 \text{GPa}$, $C_{55} = 77.76 \text{GPa}$, $C_{66} = 78.34 \text{GPa}$, the first ten frequencies from the sphere with radius = 0.893 mm are shown in Table 7. It is almost the same results given by Oda[17].

Table 5. Vibration modes of the BK-7 glass ellipsoid with different sizes.



(continued)

**Table 6.** A comparison of frequencies of ellipsoids from calculation and measurement.

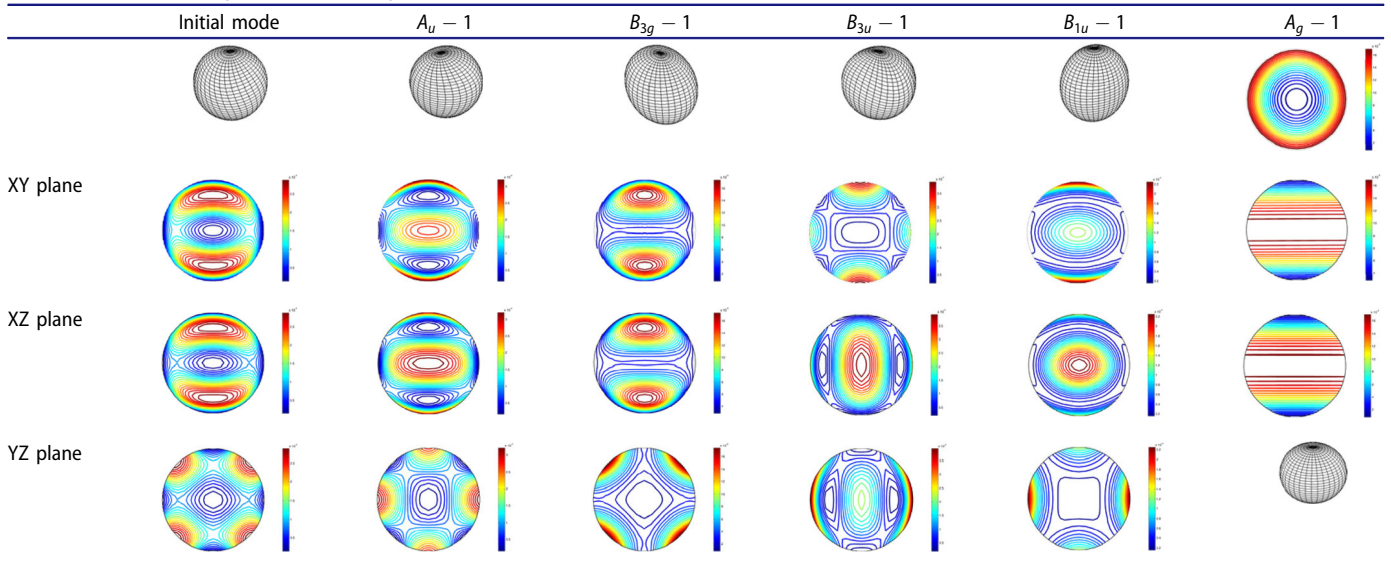
Properties of the ellipsoids	Frequency	RUSpec (kHz)	This study(kHz)	Errors
$a = 1.074\text{mm}, b = 1.07\text{mm}, c = 0.801\text{mm}, E = 1.401\text{GPa}, \nu = 0.3885, \rho = 158.85\text{kg/m}^3$	1	596.53	600.96	0.743%
	2	749.56	719.77	3.974%
	3	750.80	739.70	1.478%
	4	810.58	811.95	0.169%
$a = 1.083\text{mm}, b = 1.08\text{mm}, c = 0.763\text{mm}, E = 1.3990\text{GPa}, \nu = 0.3985, \rho = 155.85\text{kg/m}^3$	1	584.19	589.64	0.924%
	2	749.37	723.48	3.455%
	3	755.48	744.23	1.489%
	4	755.96	757.74	0.235%
$a = 1.092\text{mm}, b = 1.035\text{mm}, c = 0.79\text{mm}, E = 138.49\text{GPa}, \nu = 0.3996, \rho = 161.25\text{kg/m}^3$	1	584.19	592.54	1.409%
	2	753.89	714.15	5.271%
	3	755.48	760.89	0.711%
	4	805.09	803.10	0.247%
$a = 1.08\text{mm}, b = 1.08\text{mm}, c = 0.795\text{mm}, E = 138.89\text{GPa}, \nu = 0.3896, \rho = 158.87\text{kg/m}^3$	1	592.98	590.17	0.474%
	2	755.16	711.68	5.758%
	3	757.31	734.75	2.979%
	4	809.29	809.02	0.033%
$a = 1.078\text{mm}, b = 1.06\text{mm}, c = 0.805\text{mm}, E = 139.89\text{GPa}, \nu = 0.3812, \rho = 157.39\text{kg/m}^3$	1	606.81	608.26	0.238%
	2	761.80	738.85	3.013%
	3	761.92	754.66	0.953%
	4	815.56	814.60	0.118%

Table 7. A comparison of natural frequencies of an olivine sphere.

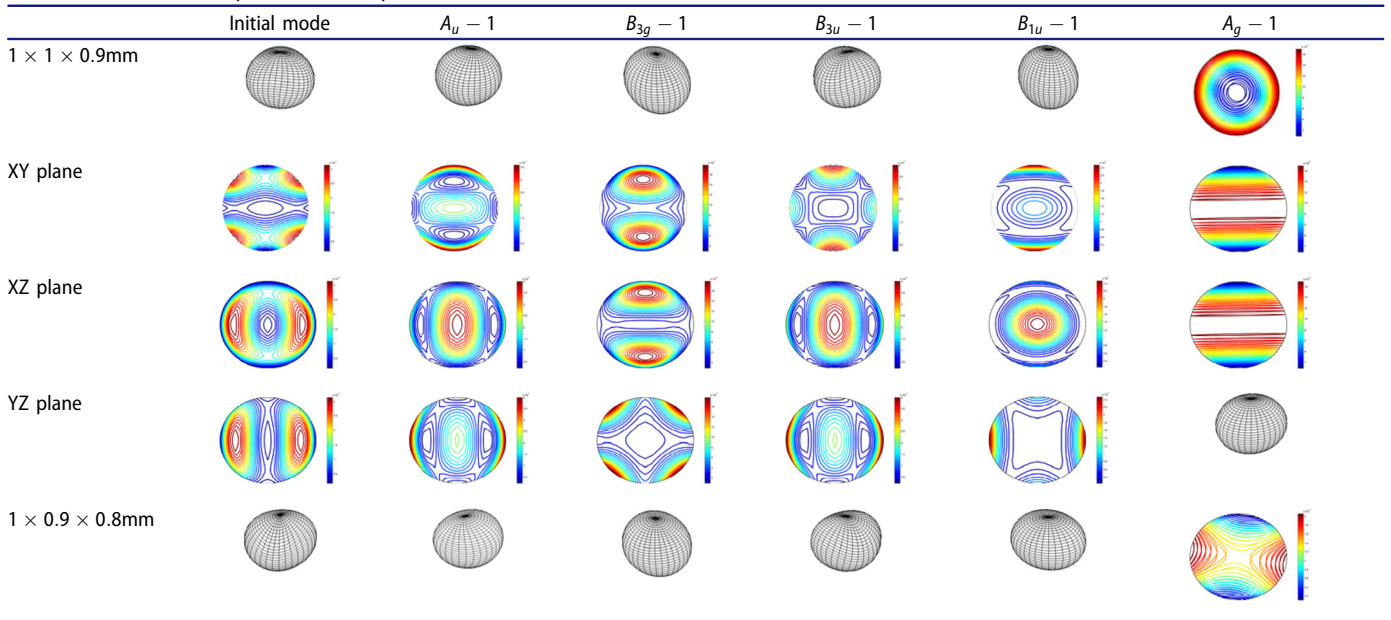
k	Modes	This study $f(\text{kHz})$	Oda [17] $f(\text{kHz})$
1	$A_u - 1$	2025	2025
2	$B_{3g} - 1$	2082	2082
3	$B_{3u} - 1$	2083	2083
4	$B_{1u} - 1$	2135	2135
5	$A_u - 2$	2140	2140
6	$A_g - 1$	2159	2159
7	$B_{2u} - 1$	2225	2225
8	$B_{2g} - 1$	2254	2254
9	$B_{1g} - 1$	2271	2271
10	$A_g - 2$	2588	2588

3.4. The natural frequency of an anisotropic ellipsoid

The above sections show that the repeated frequencies for BK-7 glass spheres with radius of 1 mm and olivine spheres of radius of 0.893 mm (Tables 2 and 7) are accurate. Now it is shown that there are indeed correct degeneracies which can be identified by looking at the frequencies of ellipsoids close to spheres. Then, the first ten frequencies from the ellipsoids of different sizes with the same material in the last part are shown in Table 9.

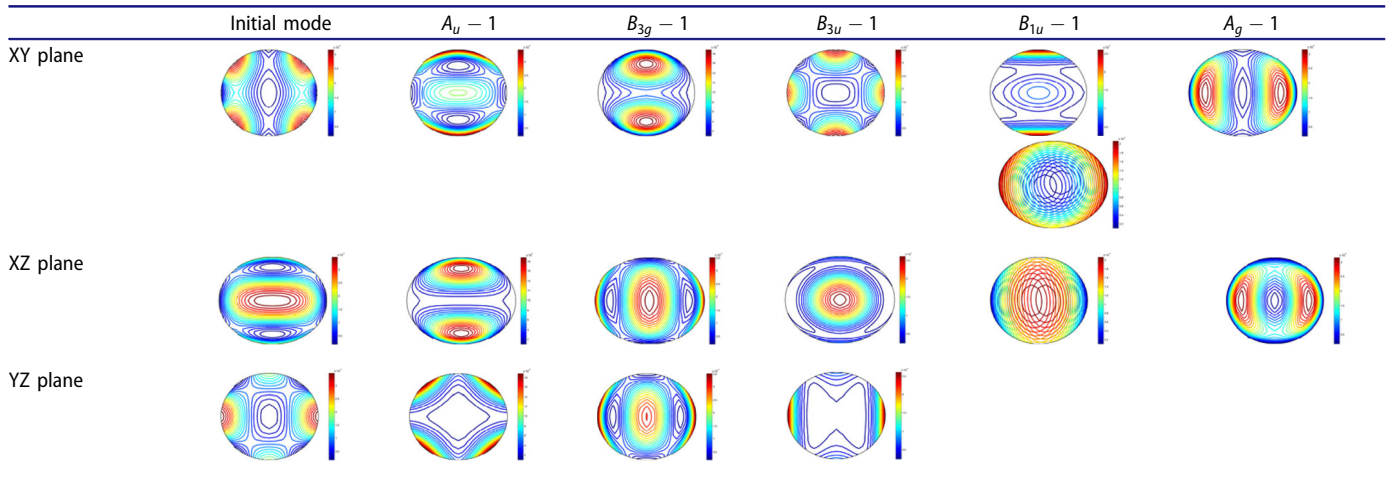
Table 8. Some mode shapes of the olivine sphere.

Table 9. The natural frequencies of olivine ellipsoids in two sizes.

k	Modes	$a \times b \times c 1 \times 1 \times 0.9$ mm f (kHz)		Modes	$a \times b \times c 1 \times 0.9 \times 0.8$ mm f (kHz)	
		Rayleigh-Ritz method	COMSOL		Rayleigh-Ritz method	COMSOL
1	$A_u - 1$	1822	1821	$A_u - 1$	1882	1881
2	$B_{1u} - 1$	1852	1853	$B_{1u} - 1$	1961	1963
3	$B_{3g} - 1$	1945	1944	$B_{3u} - 1$	2163	2163
4	$B_{3u} - 1$	1955	1955	$B_{1g} - 1$	2178	2173
5	$A_g - 1$	1990	1990	$A_g - 1$	2187	2189
6	$A_u - 2$	2031	2031	$B_{2u} - 1$	2217	2215
7	$B_{1g} - 1$	2050	2048	$B_{3g} - 1$	2226	2225
8	$B_{2g} - 1$	2112	2113	$B_{2g} - 1$	2269	2269
9	$B_{2u} - 1$	2149	2147	$A_u - 2$	2271	2272
10	$A_g - 2$	2403	2401	$A_g - 2$	2552	2549

Table 10. Some mode shapes of olivine ellipsoids.


(continued)

Table 10. Continued.



4. Conclusions

In this article, the Rayleigh–Ritz method is used to analyze the free vibrations of spherical specimens for the natural frequencies and mode shapes. The relationship between normalized frequencies and Poisson’s ratio of isotropic elastic spherical specimens is different in spherical and ellipsoidal samples, as it is found from calculations. The different modes have different behaviors with the changes of ellipsoidal parameters, and the higher frequency modes are less insensitive with the variations of the semiaxes a , b , and c . The vibration modes of anisotropic samples, on the other hand, are much less dependent on dimensions, and the individual mode shapes have distinctive characteristics that can be distinguished by the modal contours of each cross-section. In summary, the Rayleigh–Ritz method is simple and efficient for the analysis of vibrations of elastic ellipsoids, and the results converge quickly and accurately. The Chebyshev polynomials are chosen for their stability as basis functions for the displacements are easy to calculate and accurate in both frequency and modal shapes. As validated, the procedure can be used for the analysis of anisotropic ellipsoids encountered frequently in engineering applications and measurement with the resonant ultrasound spectroscopy (RUSpec) technology.

Acknowledgments

The authors acknowledge TXC-NBU Joint Center of Research receives funding from TXC (Ningbo) Corporation to promote research work for the advances of technology of acoustic wave resonators and applications. The authors are also grateful to Shining3D Company (Yangzhou, Jiangsu Province, China) for the ellipsoid samples with their excellent 3D printing technology.

Authors’ contributions

Conception, revision, and submission of the article were done by Ji Wang (JW) and Jinghui Wu (JHW), while the mathematical formulation, procedure, derivation, calculation, and check were made by RW, LX, TM, and AZ with help from JD and SZ. Reviews and discussions of the study and drafting were also shared and communicated with all

authors. All authors have read and agreed to the published this version of the manuscript.

Funding

This research was supported by the National Natural Science Foundation of China (Grant Nos. 11672142, 11772163, and 12172183) with additional support through the Technology Innovation 2025 Program (Grant 2019B10122) of the Municipality of Ningbo, Zhejiang Province, China.

ORCID

Jinghui Wu  <http://orcid.org/0000-0002-9956-1275>
Ji Wang  <http://orcid.org/0000-0002-0724-7538>

Data availability statement

The data of this study are available from authors and author’s website.

Disclosure statement

The funders and other parties had no role in the design of the study; in the collection, analyses, or interpretation of data; in the writing of the manuscript; or in the decision to publish the results.

References

- [1] D. V. Guzatov, V. V. Klimov, and M. Y. Pikhota, Plasmon oscillations in ellipsoid nanoparticles: Beyond dipole approximation, *Laser Phys.*, vol. 20, no. 1, pp. 85–99, 2010. DOI: 10.1134/S1054660X09170083.
- [2] C. X. Li, R. P. Zou, D. Pinson, A. B. Yu, and Z. Y. Zhou, An experimental study of packing of ellipsoids under vibrations, *Powder Technol.*, vol. 361, pp. 45–51, 2020. DOI: 10.1016/j.powtec.2019.10.115.
- [3] I. F. Kirichok, Numerical solution of problems of the electroelastic oscillation of a cylinder and a sphere, *Sov. Appl. Mech.*, vol. 16, no. 2, pp. 121–125, 1980. DOI: 10.1007/BF00885103.
- [4] G. R. Buchanan and G. R. Ramirez, A note on the vibration of transversely isotropic solid spheres, *J. Sound Vib.*, vol. 253, no. 3, pp. 724–732, 2002. DOI: 10.1006/jsvi.2001.4054.
- [5] D. Li, L. Dong, and R. S. Lakes, The resonant ultrasound spectroscopy method for determining the Poisson’s ratio of spheres

- over the full range, *Mater. Lett.*, vol. 143, pp. 31–34, 2015. DOI: [10.1016/j.matlet.2014.12.080](https://doi.org/10.1016/j.matlet.2014.12.080).
- [6] H. M. Wang and H. J. Ding, Radial vibration of piezoelectric/magnetostrictive composite hollow sphere, *J. Sound Vib.*, vol. 307, no. 1–2, pp. 330–348, 2007. DOI: [10.1016/j.jsv.2007.07.006](https://doi.org/10.1016/j.jsv.2007.07.006).
- [7] A. Yaoita, T. Adachi, and A. Yamaji, Determination of elastic moduli for a spherical specimen by resonant ultrasound spectroscopy, *NDT E Int.*, vol. 38, no. 7, pp. 554–560, 2005. DOI: [10.1016/j.ndteint.2005.01.010](https://doi.org/10.1016/j.ndteint.2005.01.010).
- [8] I. A. Abbas, Analytical Solution for a free vibration of a thermo-elastic hollow sphere, *Mech. Based Des. Struct. Mach.*, vol. 43, no. 3, pp. 265–276, 2015. DOI: [10.1080/15397734.2014.956244](https://doi.org/10.1080/15397734.2014.956244).
- [9] Y. Sakellariadis, Spherical functions on spherical varieties, *Am. J. Math.*, vol. 135, no. 5, pp. 1291–1381, 2013. DOI: [10.1353/ajm.2013.0046](https://doi.org/10.1353/ajm.2013.0046).
- [10] S. Ilanko, L. E. Monterrubio, and Y. Mochida, The Rayleigh–Ritz method for structural analysis, John Wiley & Sons, Ltd., London (UK) and Hoboken (USA), 2014.
- [11] D. Shahgholian, M. Safarpour, A. R. Rahimi, and A. Alibeigloo, Buckling analyses of functionally graded graphene-reinforced porous cylindrical shell using the Rayleigh–Ritz method, *Acta Mech.*, vol. 231, no. 5, pp. 1887–1902, 2020. DOI: [10.1007/s00707-020-02616-8](https://doi.org/10.1007/s00707-020-02616-8).
- [12] D. Wang, Z. C. Yang, and Z. G. Yu, Minimum stiffness location of point support for control of fundamental natural frequency of rectangular plate by Rayleigh–Ritz method, *J. Sound Vib.*, vol. 329, no. 14, pp. 2792–2808, 2010. DOI: [10.1016/j.jsv.2010.01.034](https://doi.org/10.1016/j.jsv.2010.01.034).
- [13] C. Ye and Y. Q. Wang, On the use of Chebyshev polynomials in the Rayleigh–Ritz method for vibration and buckling analyses of circular cylindrical three-dimensional graphene foam shells, *Mech. Based Des. Struct. Mach.*, vol. 49, no. 7, pp. 932–946, 2021. DOI: [10.1080/15397734.2019.1704776](https://doi.org/10.1080/15397734.2019.1704776).
- [14] J. Wang, The extended Rayleigh–Ritz method for an analysis of nonlinear vibrations, *Mech. Adv. Mater. Struct.*, vol. 3, pp. 1–4, 2021. DOI: [10.1080/15376494.2021.1892888](https://doi.org/10.1080/15376494.2021.1892888).
- [15] S. Hosseini-Hashemi and J. S. Anderson, Orthogonality and normalization of torsional modes of vibration of solid elastic spheres, *J. Sound Vib.*, vol. 121, no. 3, pp. 511–524, 1988. DOI: [10.1016/S0022-460X\(88\)80373-0](https://doi.org/10.1016/S0022-460X(88)80373-0).
- [16] F. Deneuville, M. Duquennoy, M. Ouaftouh, F. Jenot, M. Ourak, and S. Desvaux, Elastic characterization of ceramic balls using resonant ultrasound spectroscopy of spheroidal modes, *J. Acoust. Soc. Am.*, vol. 123, no. 5, pp. 3691–3691, 2008. DOI: [10.1121/1.2935073](https://doi.org/10.1121/1.2935073).
- [17] H. Oda, Aspherical correction for free vibration of elastically anisotropic solid by means of the XYZ algorithm, *PAGEOPH*, vol. 147, no. 4, pp. 719–727, 1996. DOI: [10.1007/BF01089698](https://doi.org/10.1007/BF01089698).
- [18] E. Carrera, F. A. Fazzolari, and L. Demasi, Vibration analysis of anisotropic simply supported plates by using variable kinematic and Rayleigh–Ritz method, *J. Vib. Acoust.*, vol. 133, no. 6, pp. 061017, 2011.
- [19] Y. Kumar, The Rayleigh–Ritz method for linear dynamic, static and buckling behavior of beams, shells and plates: A literature review, *J. Vib. Control.*, vol. 24, no. 7, pp. 1205–1227, 2018. DOI: [10.1177/1077546317694724](https://doi.org/10.1177/1077546317694724).
- [20] Y. Li and Y. Fu, Reliability analysis for the stability of piezoelectric delaminated axisymmetric laminated cylindrical shells, *Mech. Adv. Mater. Struct.*, vol. 21, no. 4, pp. 284–292, 2014. DOI: [10.1080/15376494.2012.680674](https://doi.org/10.1080/15376494.2012.680674).
- [21] R. Lal and Y. Kumar, Transverse vibrations of nonhomogeneous rectangular plates with variable thickness, *Mech. Adv. Mater. Struct.*, vol. 20, no. 4, pp. 264–275, 2013. DOI: [10.1080/15376494.2011.584273](https://doi.org/10.1080/15376494.2011.584273).
- [22] Z. Jing, Q. Sun, Y. Zhang, and K. Liang, Fundamental frequency maximization of composite rectangular plates by sequential permutation search algorithm, *Mech. Adv. Mater. Struct.*, pp. 1–17, 2021. DOI: [10.1080/15376494.2021.1934762](https://doi.org/10.1080/15376494.2021.1934762).
- [23] X. Shi, C. Li, F. Wang, and F. Wei, A unified formulation for free transverse vibration analysis of orthotropic plates of revolution with general boundary conditions, *Mech. Adv. Mater. Struct.*, vol. 25, no. 2, pp. 87–99, 2018. DOI: [10.1080/15376494.2016.1255823](https://doi.org/10.1080/15376494.2016.1255823).
- [24] J. Q. Gan, Z. Y. Zhou, and A. B. Yu, Structure analysis on the packing of ellipsoids under one-dimensional vibration and periodic boundary conditions, *Powder Technol.*, vol. 335, pp. 327–333, 2018. DOI: [10.1016/j.powtec.2018.05.032](https://doi.org/10.1016/j.powtec.2018.05.032).
- [25] H. B. McClung, Asymmetric vibrations of an elastic sphere, *J. Elasticity.*, vol. 25, no. 1, pp. 75–94, 1991. DOI: [10.1007/BF00041702](https://doi.org/10.1007/BF00041702).
- [26] P. J. Schafbuch, F. J. Rizzo, and R. B. Thompson, Eigenfrequencies of an elastic sphere with fixed boundary conditions, *J. Appl. Mech.*, vol. 59, no. 2, pp. 458–459, 1992. DOI: [10.1115/1.2899545](https://doi.org/10.1115/1.2899545).
- [27] H. Oda, S. Isoda, Y. Inouye, and I. Suzuki, Elastic constants and anelastic properties of an anisotropic periclase sphere as determined by the resonant sphere technique, *J. Geophys. Res.*, vol. 99, no. B8, pp. 15517, 1994. DOI: [10.1029/94JB01017](https://doi.org/10.1029/94JB01017).
- [28] D. Zhou, Y. K. Cheung, F. T. K. Au, and S. H. Lo, Three-dimensional vibration analysis of thick rectangular plates using Chebyshev polynomial and Ritz method, *Int. J. Solids Struct.*, vol. 39, no. 26, pp. 6339–6353, 2002. DOI: [10.1016/S0020-7683\(02\)00460-2](https://doi.org/10.1016/S0020-7683(02)00460-2).
- [29] I. Kim, M. Song, and J. Kim, Effects of Ti–B and Si additions on microstructure and mechanical properties of Al–Cu–Mg based aluminum matrix composites, *J. Alloys Compd.*, vol. 832, pp. 154827, 2020. DOI: [10.1016/j.jallcom.2020.154827](https://doi.org/10.1016/j.jallcom.2020.154827).
- [30] J. Maynard, Resonant ultrasound spectroscopy, *Phys. Today.*, vol. 49, no. 1, pp. 26–31, 1996. DOI: [10.1063/1.881483](https://doi.org/10.1063/1.881483).
- [31] M. Janovská, P. Sedlák, A. Kruisová, H. Seiner, M. Landa, and J. Grym, Elastic constants of nanoporous III–V semiconductors, *J. Phys. D: Appl. Phys.*, vol. 48, no. 24, pp. 245102, 2015. DOI: [10.1088/0022-3727/48/24/245102](https://doi.org/10.1088/0022-3727/48/24/245102).
- [32] P. Sedlák, H. Seiner, L. Bodnárová, O. Heczko, and M. Landa, Elastic constants of non-modulated Ni–Mn–Ga martensite, *Scr. Mater.*, vol. 136, pp. 20–23, 2017. DOI: [10.1016/j.scriptamat.2017.03.041](https://doi.org/10.1016/j.scriptamat.2017.03.041).
- [33] H. Oda, J. Hirao, I. Suzuki, W. M. Visscher, and O. L. Anderson, Free oscillations of elastically anisotropic spheres and ellipsoids, *Geophys. J. Int.*, vol. 118, no. 3, pp. 555–565, 1994. DOI: [10.1111/j.1365-246X.1994.tb03984.x](https://doi.org/10.1111/j.1365-246X.1994.tb03984.x).
- [34] D. Zhou, F. T. K. Au, Y. K. Cheung, and S. H. Lo, Three-dimensional vibration analysis of circular and annular plates via the Chebyshev–Ritz method, *Int. J. Solids Struct.*, vol. 40, no. 12, pp. 3089–3105, 2003. DOI: [10.1016/S0020-7683\(03\)00114-8](https://doi.org/10.1016/S0020-7683(03)00114-8).